buildings

MDPI

Article

Data-Driven Model-Based Control Strategies to Improve the Cooling Performance of Commercial and Institutional Buildings

Etienne Saloux * and Kun Zhang

CanmetENERGY, Natural Resources Canada, Varennes, QC J3X 1P7, Canada
* Correspondence: etienne.saloux@nrcan-rncan.gc.ca

Abstract: The increasing amount of operational data in buildings opens up new methods for improving building performance through advanced controls. Although predictive control has been widely investigated in the literature, field demonstrations still remain rare. Alternatively, model-based controls can provide similar improvement while being easier to implement in real buildings. This paper investigates three data-driven model-based control strategies to improve the cooling performance of commercial and institutional buildings: (a) chiller sequencing, (b) free cooling, and (c) supply air temperature reset. These energy efficiency measures are applied to an existing commercial building in Canada with data from summer 2020 and 2021. The impact of each measure is individually assessed, as well as their combined effects. The results show that all three of the measures together reduce building cooling energy by 12% and cooling system electric energy by 33%.

Keywords: advanced controls; energy efficiency; model-based controls; free cooling; chiller sequencing; temperature reset strategies

check for updates

Citation: Saloux, E.; Zhang, K. Data-Driven Model-Based Control Strategies to Improve the Cooling Performance of Commercial and Institutional Buildings. *Buildings* **2023**, *13*, 474. https://doi.org/10.3390/buildings13020474

Academic Editors: Christopher Yu-Hang Chao and Kian Jon Chua

Received: 5 January 2023
Revised: 26 January 2023
Accepted: 7 February 2023
Published: 9 February 2023

Copyright: © 2023 by the authors. Licensee MDPI, Basel, Switzerland. This article is an open access article distributed under the terms and conditions of the Creative Commons Attribution (CC BY) license (https://creativecommons.org/licenses/by/4.0/).

1. Introduction

1.1. Motivation

Despite the efforts made toward control optimization, most existing buildings are still not operated at a high level of energy efficiency. It is estimated that the annual energy use of existing buildings could be reduced by up to 30% [1] with the improvement of control and operation, as well as the detection and correction of equipment problems and inefficiencies [2]. Besides energy savings, more efficient building operation could reduce maintenance costs by 20% [3]. Furthermore, with the advent of increasingly efficient technologies, buildings are becoming more and more complex. Thus, the adequate optimization of building operation has become a key enabler for harvesting the full potential of these energy systems. Kramer et al. [4] conducted a vast campaign to prove the business case for building analytics. They categorized commercial products that are available on the market for optimizing building controls into three categories: energy information system, fault detection and diagnostics, and automated system optimization. They tested 85 different software on 6500 buildings from 104 organizations and showed that the median annual energy savings could reach up to 9% with a two-year simple payback.

Moreover, sub-hourly data have become increasingly available in buildings and provide an untapped opportunity for improving existing building controls. This vast amount of data could be leveraged to support the development of advanced control strategies, which could eventually be further integrated into existing building automation systems (BAS) or building optimization commercial platforms. Model-based predictive controls (MPC) are a compelling example and have been intensively investigated in the past decades [5]. This method consists of the use of a control-oriented model along with forecasts (e.g., weather, occupancy) to predict the future behavior of a building hours ahead and optimize its heating and cooling system operation accordingly. Although it shows good promise in theory, its implementation in existing buildings remains relatively scarce and somewhat

challenging [6,7]. On the other hand, operational data could still be leveraged through simpler approaches such as data-driven rule- or model-based controls, which are much easier to implement in existing buildings.

This paper aims to investigate three data-driven model-based control strategies, which can be readily implemented in actual building controls to improve the cooling performance of Commercial and Institutional (CI) buildings equipped with BAS.

1.2. Literature Review

Various control strategies for optimizing building operation have been investigated in the past and inventoried in review papers. For instance, Wang and Ma [8] investigated supervisory and optimal control for building Heating, Ventilation and Air Conditioning (HVAC) systems while Afram and Janabi-Sharifi [9], and more recently Taheri et al. [10], conducted reviews of MPC strategies for HVAC systems. In addition, some authors focused on specific aspects of building operation. Thieblemont et al. [11] and Yu et al. [12] investigated MPC for buildings equipped with energy storage devices. Péan et al. [13] reviewed control strategies for heat pump systems for enhancing flexibility. Darwazeh et al. concentrated on peak load management strategies [14]. Finally, Mirakhorli and Dong [15] focused on occupancy behavior-based MPC while Park et al. [16] conducted a review of field implementations of occupant-centric building controls. Although a good proportion of these publications focus on applications related to building heating performance, advanced controls have also been widely used for improving the cooling performance. Some of these applications include, among others:

- Building precooling in a time-of-use tariff structure, targeting the reduction of building energy use during mid-peak and high-peak hours [17].
- The optimization of HVAC operating conditions, targeting the reduction of building energy use [18] or building electric power [19].
- The optimization of fresh air intake based on occupancy, aiming to provide a suitable amount of fresh air depending on the actual number of occupants [20].
- Natural and hybrid ventilation, targeting the incorporation of more fresh air into the building at critical times of the day to reduce mechanical cooling [21,22].
- The optimization of cooling system performance, with the goal of improving the chiller performance at the part-load ratio [23–25].
- The management of ice banks, targeting the reduction of building energy use during peak hours [26–28].
- The management of radiant slab systems to reduce building energy use in the morning while improving thermal comfort [29,30].

Three applications are further discussed since they are the foundations of the proposed measures: local HVAC controls, chilled water system performance at the part-load ratio, and free cooling.

Recently, ASHRAE Guideline 36 (G36) has been released and provides high-performance control sequences to improve the operation of HVAC systems [31]. Such standardized control sequences will help reduce engineering time and reduce programming and commissioning time while improving energy efficiency and indoor air quality. This guideline has focused on airside equipment, mainly variable air volume (VAV) systems and terminal units, as well as more recently, on waterside equipment related to heating and cooling plants. Zhang et al. [18] estimated the potential savings obtained by retrofitting existing controls to new control sequences based on this guideline and applied it to multi-zone VAV systems. They tested various scenarios under different climates, building operating hours, and internal load magnitudes, and found that G36 control sequences could reduce energy use by 2–75% with an average of 31%. Three control strategies played a significant role in this reduction: supply air temperature reset, duct static pressure reset, and zone airflow control.

For the cooling system operation at the part-load ratio, Thangavelu et al. [23] investigated a multi-chiller plant and evaluated its electric power as the contribution of that

of the chiller, the circulating pumps, and the cooling tower fans. They proposed a novel methodology, which optimizes the flowrates of chilled and condenser water, chilled and condenser water temperatures, and cooling tower air flowrates, to maximize cooling system performance. They validated the approach using three case studies and found that the energy savings could reach 20%, 40%, and 42%, respectively, compared to conventional controls. Fan et al. [32] studied optimal control strategies for a multi-chiller system to determine the optimal sequencing based on probability density distribution of the cooling load ratio. They obtained savings of up to 4% compared to the original control strategy. Liao and Huang [24] developed a hybrid predictive sequencing control for a multi-chiller plant, which optimizes the chiller sequencing based on the forecasted cooling load. For this purpose, chiller performance curves were derived from three months of historical data from a real chiller and the objective function was intended to enhance system stability (i.e., number of chiller switches) and reduce operational costs while maintaining thermal comfort and energy efficiency. It is worth mentioning that operational costs were calculated as the sum of the chiller plant energy consumption, the start-up cost of chiller plants (chillers and pumps), and the depreciation cost of all devices. The results showed that the switch number of chillers was reduced by 20% and the operational cost decreased by 4%. A similar approach was developed by Gunay et al. [25] for equipment sequencing in a central heating and cooling plant. The hourly cooling peak load was forecasted for the next day and the chiller sequencing was adjusted accordingly. Operational data were used to derive data-driven performance curves for the five chillers of the cooling plant. The authors obtained cooling energy savings of 25% compared to the current operation. The importance of chiller scheduling has also been reported by Chen et al. [33]. The authors studied the impact of multi-chiller plants on design and operation optimization and considered 13 centrifugal chillers. They showed that it is a good practice to select chillers with different capacities and that energy consumption could be reduced by 20% with the best chiller design option compared with the worst option.

Free cooling is an effective strategy to improve HVAC system performance when outdoor air conditions are favorable. Broadly speaking, "free cooling" strategies can be implemented in various ways such as by using airside and waterside economizers, or natural and hybrid ventilation. An airside economizer increases fresh air intake and reduces the return air by adjusting the dampers in the air handling unit (AHU) system. ASHRAE Standard 90.1 specifies various operating conditions for economizer high limits and devices (e.g., fixed and/or differential dry bulb or enthalpy) [34]. Hybrid ventilation offers a great opportunity for taking advantage of favorable outdoor air conditions to precool buildings at night in order to discharge building thermal mass, which decreases operative temperature, and to reduce mechanical cooling during the day [22]. A hybrid ventilation system consists of a possibly fan-assisted system (e.g., windows and motorized dampers), which allows the outdoor air to enter the building and that is used along with a mechanical cooling system (e.g., chillers) to provide cooling to the building at all times [21]. Stasi et al. [35] investigated nearly zero-energy buildings three hybrid ventilation strategies: earth-to-air heat exchanger, night hybrid ventilation, and free cooling mode, and showed that cooling energy was reduced by 14–21%, and electricity consumption by 8%, respectively.

1.3. Paper Objectives and Contributions

This paper intends to develop and evaluate energy efficiency measures to improve the cooling system performance of CI buildings. Specifically, these measures are:

- Chiller sequencing based on data-driven performance curves;
- Free cooling strategy based on electric power estimation of the whole cooling system, including both the waterside (chilled water system) and airside system (AHUs);
- Supply air temperature reset strategies.

The contributions of the paper include the following:

- The proposed measures build upon operational data, virtual energy meters, and control-oriented models, which do not require prediction and forecasting, and aim

to be readily implementable in existing buildings while being more robust and less prone to errors compared to more complex methods such as model predictive control.

- The proposed measures tackle the existing systems and do not require the installation of additional equipment (e.g., sensors, meters, motorized operable windows for natural ventilation, etc.). The implementation only requires minimum code modification in the BAS, making it applicable to a wide range of CI buildings with different HVAC configurations.
- This work evaluates both the individual and combined impacts of energy efficiency measures in the same building, which has rarely been investigated in the past to the best of our knowledge.

The paper is organized as follows: Section 2 describes the case study, an existing large commercial building. The three proposed measures are described in Section 3, where the methodology to assess the performance is also explained. Section 4 reports the performance of each measure, as well as their combined performance, and discusses the generalizability of the measures. Section 5 concludes the paper.

2. Case Study: A Large Commercial Building

2.1. Building Description

The case study building is a 36,000-m^2, 11-floor commercial building located in Montreal, Quebec. Figure 1 shows a schematic of the chilled water network. The cooling plant is composed of three chillers: one centrifugal chiller connected to two wet cooling towers and two screw chillers connected to two air-cooled condensers or dry cooling towers. A heat exchanger is connected to the condenser water network of the air-cooled condensers as a waterside economizer. It is activated when the outdoor air temperature is low. The chilled water is distributed to cooling coils in the AHUs which are located on different floors of the building.

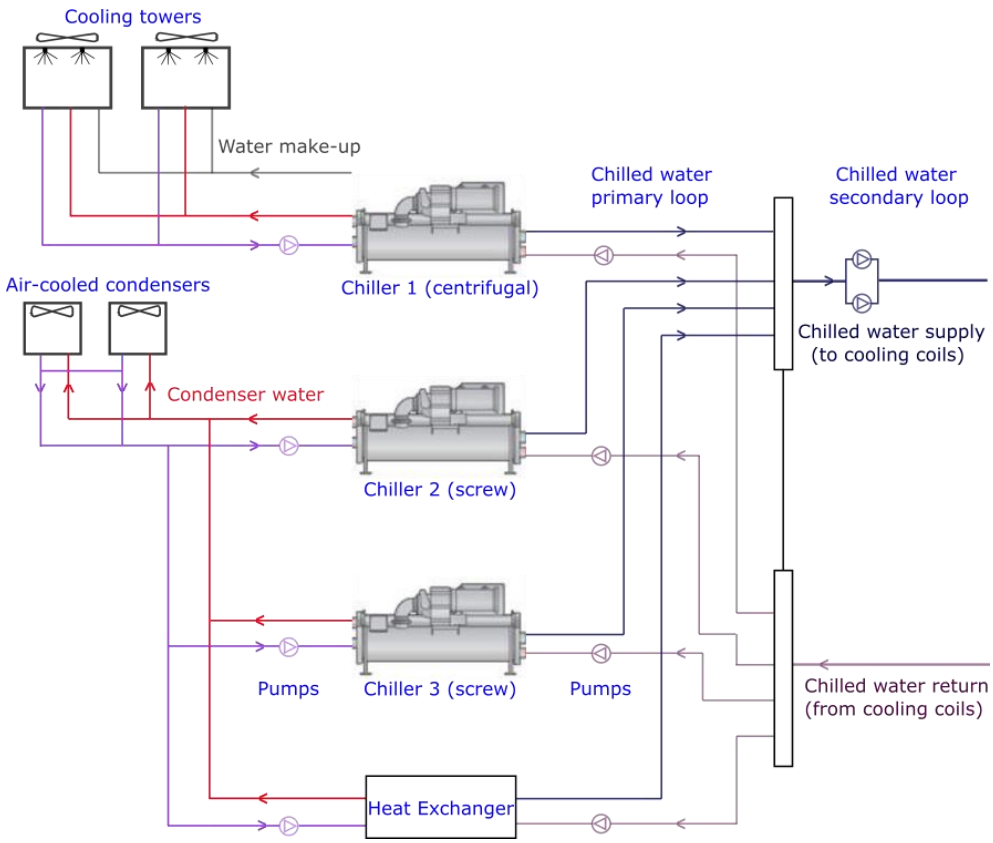

Figure 1. Schematic of the chilled water system in the large commercial case study building.

The airside system is a primary-secondary AHU system. The primary AHU system is composed of two fresh air pre-treatment units equipped with gas burners, precooling coils, humidifiers, and heat recovery wheels to pre-treat the outdoor air before being sent to the secondary AHU system. This secondary system consists of 22 cooling coils in the AHU located from the 2nd floor to the 11th floor. Once conditioned in the primary AHU system, the outdoor air is mixed with the return air in each AHU in the different floors, further cooled down if required, and discharged to building zones through single- or dual-duct systems. For dual-duct systems, a fraction of the cooled air flowrate is bypassed via the hot deck before being mixed again with the cold deck. Figure 2 shows a schematic of the air handling unit system.

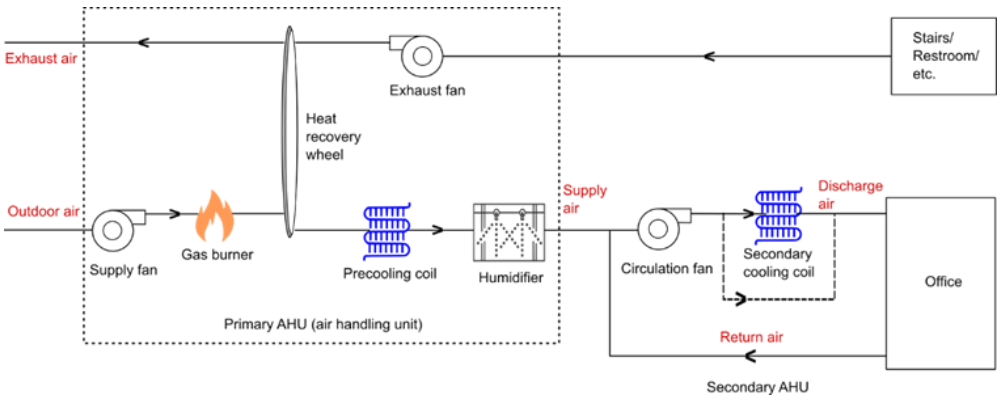

Figure 2. Schematic of the air handling unit system in the large commercial case study building [36].

2.2. Operational Data

Building operational data such as temperature, relative humidity, pressure, flow rates, valve openings, chiller modulation, and electric currents (amps) were recorded at five-min intervals. More specifically, the following variables were used for the modelling and calculations:

- *Primary loop of chilled water network*: amps of circulation pumps;
- *Secondary loop of chilled water network*: flowrate along with supply and return water temperature to estimate building cooling load; amps of circulation pumps;
- *Chillers*: % Rated Load Amps (RLA) for each chiller, used to derive electric power;
- *Condenser water loop:* amps of fans in cooling towers and air-cooled condensers; amps of circulation pumps;
- *Air handling units*: supply and discharged air temperatures; outdoor air temperature and relative humidity; return air temperature and relative humidity; air flowrates; amps from the fans.

The data collected from 1 June 2020 to 1 September 2020 and from 1 June 2021 to 1 September 2021 were used to develop and validate the proposed data-driven measures. The outliers and missing data were removed from the dataset based on statistical means and expert knowledge. The available data allowed for calculation of the cooling thermal power at the building level, although not at the chiller level due to the lack of measurement devices. Therefore, chiller performance curves were generated for combinations of chillers in operation and the building cooling power was used as a proxy. More information on the uncertainty analysis of the building cooling power can be found in [36]. Spot measurements were used to derive electric power from % RLA for each chiller. When spot measurements could not be collected, manufacturer specifications were used as an alternative.

2.3. Energy Use of the Building

This subsection provides an overview of the electric and thermal energy usage in the case study building, especially the contribution of chillers, pumps, and cooling towers to the building electric power and the impact of ventilation on the building cooling

load. This analysis aims to better put in perspective the potential energy savings of the proposed measures.

Figure 3 shows the electricity use of the chillers, chiller auxiliary equipment (i.e., circulation pumps, cooling tower fans, air-cooled condenser fans), the AHU fans (for both primary and secondary systems), and the remaining load, deduced from the total building electricity consumption. Note that chiller auxiliary equipment concentrates on the major energy loads (pumps and fans) and excludes the consumption of smaller loads such as valves and damper actuators. In total, the chilled water system and the AHU fans contribute 60–70% of the total building electricity use.



Figure 3. Electricity use of the case study building: "Baseload" refers to the non-HVAC load; "AHU fans" includes all of the fans in the air distribution network; "Pumps and cooling towers" refers to all the pumps in the water network and all the fans in the cooling towers and air-cooled condensers; "Chillers" include all three chillers.

A similar calculation was done for the building cooling load. Figure 4 shows the mechanical cooling load provided by the chilled water system as well as the contribution from fresh-air pretreatment, which accounts for ventilation requirements for occupancy and air quality, as well as space cooling (i.e., room conditioning), deduced from the difference between the chilled water system and fresh-air pretreatment. The fresh air pretreatment thermal power ($\dot{Q}_{\text{fresh air pretreat}}$) is calculated as follows:

$$\dot{Q}_{\text{fresh air pretreat}} = \dot{m}_{\text{fre,occ}}(h_{\text{OA}} - h_{\text{EA}}), \quad (1)$$

where $\dot{m}_{\text{fre,occ}}$ is the fresh air flowrate related to occupancy, and h_{OA} and h_{EA} are the enthalpy of outdoor air and exhaust air. A negative value means that fresh air pretreatment cools down the building by introducing cool fresh air; in contrast, a positive value means that it requires additional cooling to pretreat the air to indoor conditions. Figure 4 shows that fresh air pretreatment significantly contributes to the total cooling load, especially when it was hot and humid in July and August 2020, and August 2021. In June 2020 and 2021, and July 2021, its average was close to zero, meaning that the free cooling and cooling load introduced by the fresh air intake is approximately equal in those months.

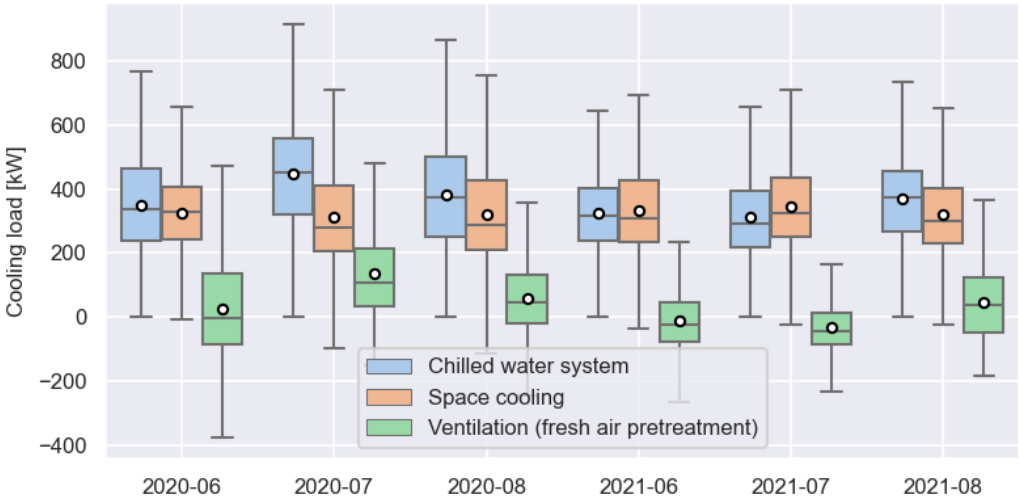

Figure 4. Cooling load overview for the case study building: the chilled water system bars show the overall cooling load incurred in the plants; the bars labelled space cooling and ventilation represent the amount of cooling load used for room conditioning and fresh air pretreatment.

3. Development of Data-Driven Measures

3.1. Chiller Sequencing

Chiller sequencing intends to take advantage of the most efficient chillers at specific cooling loads to increase the system energy efficiency. The proposed chiller sequencing is based on performance curves derived directly from the operational data. Developing performance curves based on operation data allows for capturing the performance difference between identical chillers in real-world scenarios. Manufacturer data in the chiller specifications will not be able to reflect those differences [37], whereas such differences could be further exploited to improve chilled water system performance. A similar situation was found for heat pumps [38].

3.1.1. Chilled Water System Models at Part-Load Ratio

The performance of chillers mainly depends on three factors [23]: supply water temperature at the evaporator, supply water temperature at the condenser, and the chiller part–load ratio, i.e., the ratio between the cooling load at which the chiller is operated and its nominal cooling capacity. In operation, the chiller part–load ratio appears to be the main variable that affects the system performance and has been mainly used for modelling purposes [24,25]. In fact, this simplification eases the chiller sequencing and could be justified by the slight variation in the water temperature on the demand side (evaporator) in operation, while the effect of water temperature at the condenser could be relatively well-captured by the part–load ratio itself. Indeed, if the outdoor air temperature is high, the water temperature at the condenser might be relatively high as well, which coincides with a higher cooling load and, thus, a higher chiller part–load ratio.

The chiller COP has been calculated as follows:

$$COP_{ch} = \frac{\dot{Q}_{cool}}{\sum_i \dot{W}_{\mathrm{ch},i}} = \frac{\dot{m}_{\mathrm{w}} c_{\mathrm{p,w}} \left(T_{\mathrm{ret}} - T_{\mathrm{sup}}\right)}{\sum_i \dot{W}_{\mathrm{ch},i}}, \tag{2}$$

where $\dot{Q}_{cool}$ is the building cooling load, which is estimated from water flowrate ($\dot{m}_{\mathrm{w}}$), and supply and return water temperature (T_{sup} and T_{ret}). $c_{\mathrm{p,w}}$ is the water specific heat at constant pressure. $\dot{W}_{\mathrm{ch},i}$ is the electric power of the ith chiller.

Figure 5 shows the chiller data-driven performance curves obtained using hourly averaged data. Note that the chiller COP is shown against the thermal load, not the part–load ratio, in order to support the development of the chiller sequencing strategy. The

centrifugal chiller is referred to as CH #1, while screw chillers are referred to as CH #2 and CH #3. Since the evaporator thermal power was not measured, these curves were developed only when chillers were individually in operation (i.e., one at a time) or for a given combination of chillers (e.g., both screw chillers at the same time). To generate relatively cleaned performance curves, the following data process steps were taken:

- Low differences between water supply and return temperature (<3 °C) were excluded by statistical means;
- Low water flow rates (<10 kg/s) were excluded by statistical means;
- Low hourly electric power values (<25 kW) were excluded by statistical means; this allows for avoiding possible cycling;
- To remove transient operation, for each datum point, the corresponding combination of chillers must have been in operation for one hour and must remain in operation for one hour.

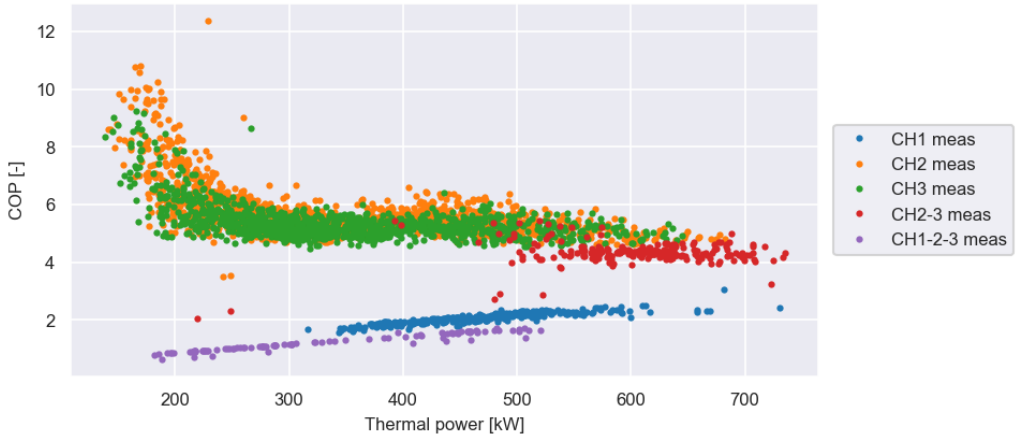

Figure 5. Chiller data-driven performance curves obtained with operational data. The electric power accounts for the chiller(s) in operation only.

The results from Figure 5 show that screw chillers (CH #2 and CH #3), although identical, have slightly different performance curves and are the most efficient units in this multi-chiller system. Both screw chillers show an unexpected COP increase at a low part–load ratio; this could be partially explained by the measurement uncertainty at a low load. When both of the screw chillers are in operation at the same time (CH #2 and #3), their combined performance is lower than when they are operated alone. This could be explained by the less-favorable operating conditions when the cooling load is high (i.e., lower inlet water temperature at the evaporator and higher inlet water temperature at the condenser). On the other hand, the centrifugal chiller (CH #1) shows an unexpected poor performance, which may indicate a technical issue. This was raised to the building technical team, which has further investigated this aspect and found that the chiller was rusted and needed in-depth cleaning. Once the chiller is cleaned, the performance curve can be easily updated to account for the new situation.

The main drawback of chiller performance curves is that they does not consider the power use of auxiliary devices, such as circulation pumps and fans from cooling towers. At a low cooling load, the chiller might be energy efficient; nonetheless, the electric power of pumps and fans might remain high. This may significantly reduce the system performance of the chilled water network. To account for the energy use from auxiliary equipment, the chilled water system COP has been calculated as follows:

$$COP_{cool} = \frac{\dot{Q}_{cool}}{\sum_i \left(\dot{W}_{\mathrm{ch},i} + \sum_j \dot{W}_{\mathrm{pp},i,j} + \sum_k \dot{W}_{\mathrm{fan},i,k} \right)}, \quad (3)$$

where $\dot{W}_{pp,i,j}$ is the electric power of the jth circulation pump related to the operation of the ith chiller; it includes pumps in both primary and secondary water loops. $\dot{W}_{fan,i,k}$ is the electric power of the kth fan related to the operation of the ith chiller; it includes fans in the air-cooled condensers and/or cooling towers.

Figure 6 shows the performance curves of the chilled water system. As expected, at a low cooling load, chiller electric power is relatively low and the contribution of auxiliary equipment to the total electric power becomes significant. Overall, similar trends were obtained: individual screw chillers perform the best, followed by the combination of screw chillers, the centrifugal chiller, and, last, all chillers together. Other chiller combinations were barely found in the historical data. In general, the auxiliary equipment significantly reduces the performance: the chilled water system COP (Figure 6) almost never exceeds 3 while the chiller COP (Figure 5) can easily reach 6 and beyond.

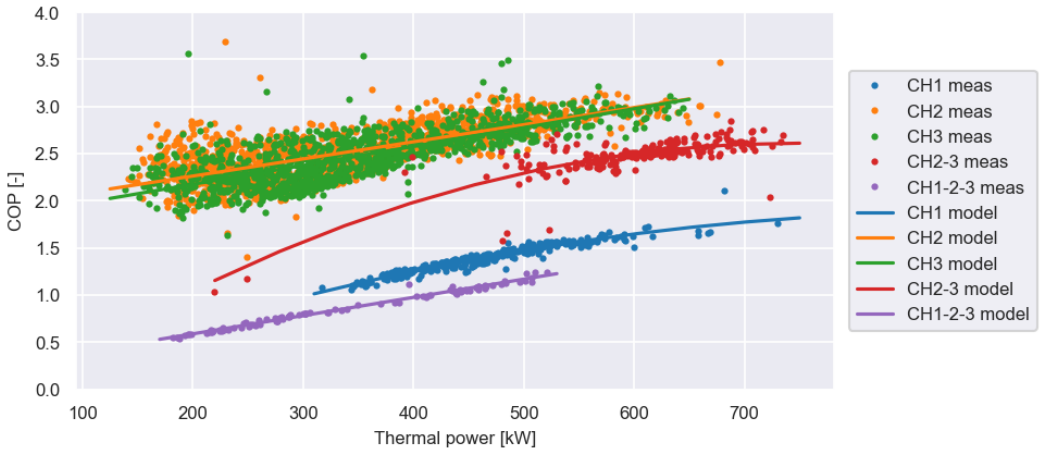

Figure 6. Chilled water system data-driven performance curves obtained with operational data. The electric power accounts for the chiller(s) in operation and the associated auxiliary equipment (i.e., circulation pumps, cooling tower fans, air-cooled condenser fans).

3.1.2. Proposed Chiller Sequencing Strategy

Chilled water system data-driven performance curves (Figure 6) were used to develop the new chiller sequencing strategy. Linear models were used to estimate the COP of the screw chillers (CH #2 and CH #3) and all of the chillers together (CH #1-3) from the thermal load; quadratic models were used for the combination of the screw chillers (CH #2-3) and the centrifugal chiller (CH #1):

$$COP_{CH\#1} = -2.375e^{-6}\dot{Q}^{2}_{CH\#1} + 4.348e^{-3}\dot{Q}_{CH\#1} - 1.068, \quad (4)$$

$$COP_{CH\#2} = 1.818e^{-3}\dot{Q}_{CH\#2} + 1.898, \quad (5)$$

$$COP_{CH\#3} = 2.004e^{-3}\dot{Q}_{CH\#3} + 1.774, \quad (6)$$

$$COP_{CH\#2\text{-}3} = -5.307e^{-6}\dot{Q}^{2}_{CH\#2\text{-}3} + 7.896e^{-3}\dot{Q}_{CH\#2\text{-}3} - 0.326, \quad (7)$$

$$COP_{CH\#1\text{-}2\text{-}3} = 1.935e^{-3}\dot{Q}_{CH\#1\text{-}2\text{-}3} + 2.009, \quad (8)$$

The model accuracy was evaluated based on the coefficient of determination (R^2), the normalized mean bias error (NMBE), and the coefficient of variation of the root mean square error (CV-RMSE) [39]. The results are given in Table 1 and show good consistency with the operational data.

Table 1. Accuracy of chilled water system COP models.

Chiller in Operation	Model	R^2	NMBE	CV-RMSE
CH #1 (centrifugal)	Quadratic	0.92	3.3×10^{-14}%	3.0%
CH #2 (screw)	Linear	0.53	2.2×10^{-14}%	7.5%
CH #3 (screw)	Linear	0.57	-2.3×10^{-14}%	7.5%
CH #2-3	Quadratic	0.61	-2.1×10^{-14}%	5.0%
CH #1-2-3	Linear	0.98	-3.5×10^{-14}%	2.9%

Based on the findings from Figure 6, it appears that CH #2 is the most efficient chiller, although the difference with CH #3 becomes negligible for a cooling load higher than 575 kW. At a high cooling load (above 650 kW), both screw chillers CH #2 and #3 might be required and should be used, instead of the centrifugal chiller. Switch-on and switch-off thresholds should also be considered to avoid cycling, while more advanced controls could be incorporated as well to reduce the number of switches and chiller start-ups [24]. For the present case study, the proposed chiller sequencing is described in Table 2. Switch-on and switch-off thresholds were tuned to reduce the number of chiller switches without degrading the system performance. The centrifugal chiller is not used in the proposed sequencing due to its poor performance.

Table 2. Chiller sequencing strategy: switch-on and switch-off thresholds.

Switch-On Threshold		Switch-Off Threshold	
From #2 to #3	575 kW	From #3 to #2	550 kW
From #3 to #2-3	650 kW	From #2-3 to #3	625 kW

Although more advanced controls could be used to improve the multi-chiller system by considering more complex chiller models [23], more control variables (e.g., water and air flowrates and temperatures) [23], or advanced optimization routines [40], the proposed approach requires limited operational data, only targets chiller sequencing without affecting local controls in the chilled water network (and related technical considerations), and relies on a simple part–load ratio model for the chillers, which eases the development of the sequencing strategy. Such features are intended to facilitate the implementation of the proposed strategy into actual control systems and the replicability to other multi-chiller systems.

3.2. Free Cooling

A free cooling strategy aims to cool down a building with or without the limited use of a mechanical device by introducing more outdoor air when conditions are favorable. Unlike conventional free cooling strategies which rely on natural or hybrid ventilation generally, the proposed free cooling strategy is to increase fresh air intake through the existing mechanical ventilation system in the AHUs. Increasing the ventilation flowrate might reduce the chilled water system electric power; however, it also increases the AHU fan power consumption, whose contribution can be significant to the total building electric power (see Section 2.3). The proposed free cooling strategy aims to identify outdoor conditions under which the total electric power of the chilled water system and the AHU fans is lower compared to the baseline operation, i.e., without increased fresh air flowrates.

3.2.1. Free Cooling Thermal Power

Quebec's climate shows a high potential for free cooling, which is mainly due to the large daily temperature variations, as temperatures at night can easily go below 15 °C [22]. Free cooling in these conditions especially occurs in early or late summer, or during shoulder seasons, and depends on required indoor air conditions.

To evaluate the feasibility of potential free cooling, outdoor air conditions must be lower than indoor air conditions. In this case, incorporating more fresh air cools down

the building. Otherwise, more cooling from the mechanical cooling system is required to pre-condition the fresh air (see Section 2.3). This fresh-air pre-treatment can be evaluated by comparing fresh air and return (or exhaust) air conditions. In addition, the amount of potential free cooling depends on the capacity of the ventilation system to incorporate more fresh air into the system, besides occupancy needs. At night, occupancy in CI buildings is relatively low, which offers more potential for free cooling than during the daytime. Consequently, the free cooling thermal power can be estimated as follows:

$$\dot{Q}_{\text{free cooling}} = \min\left(\dot{Q}_{\text{total cooling}}, (\dot{m}_{\text{fre,max}} - \dot{m}_{\text{fre,occ}})(h_{\text{OA}} - h_{\text{EA}})\right), \quad (9)$$

where $\dot{Q}_{\text{free cooling}}$ is the total building cooling load (kW), $\dot{m}_{\text{fre,max}}$ and $\dot{m}_{\text{fre,occ}}$ are the maximum fresh air flowrate based on ventilation system capacity and fresh air requirements for occupancy purposes (kg/s), and h_{OA} and h_{EA} are outdoor air and exhaust air enthalpies (kJ/kg) and depend on temperature and relative humidity. From the operational data for summer 2020 and 2021, the maximum fresh air flowrate observed was 20,500 L/s; this value was used in Equation (9). In theory, Equation (9) provides the maximum free cooling thermal power by considering the maximum fresh air flowrate. However, a more sophisticated approach could be to test all possible flow rates from occupancy requirements up to the maximum; however, it would also make the approach more complex and more difficult to implement in real buildings.

Figure 7 shows the total building cooling load and the free cooling thermal power for one week in late August 2020. It is worth mentioning that this free cooling thermal power is possible due to favorable outdoor air conditions compared to indoor air conditions, and only accounts for the free cooling potential from a thermal load viewpoint. In other words, it does not necessarily mean that it is efficient to conduct free cooling from an electric power perspective (see Section 3.2.3). We can see that free cooling is possible mainly at night, although also sometimes during the day due to lower outdoor air conditions during this period of the year. Figure 7 also shows the fresh air flowrate required for occupancy needs and the flow rate available for free cooling. During the day, building occupancy is higher and reduces the potential for free cooling by decreasing the available air flowrate for free cooling (see Equation (9)), which partially explains why the potential free cooling thermal power is lower during work hours. The total fresh air flowrate is sometimes below 20,500 L/s, which occurs when the potential free cooling load exceeds the building cooling load and is adjusted to exactly match it by lowering the flowrate.

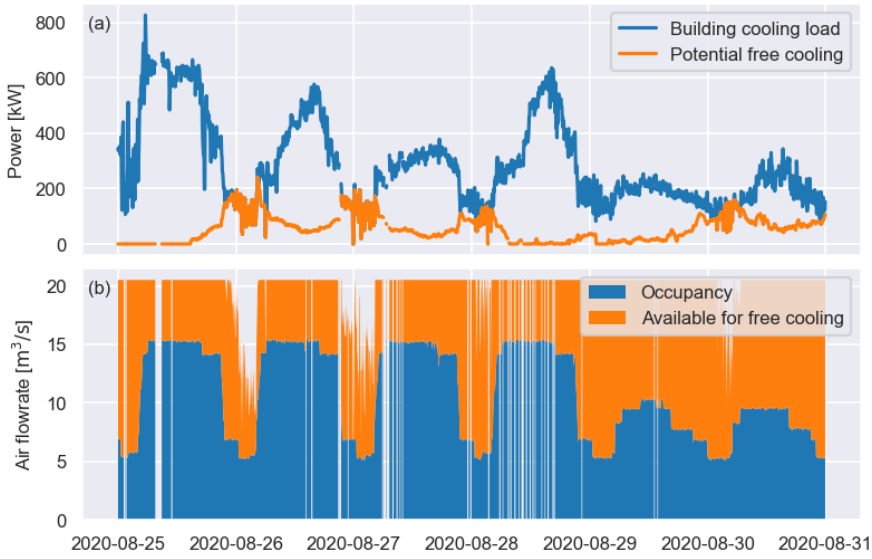

Figure 7. (**a**) Total building cooling load and free cooling thermal power, and (**b**) fresh air flowrate for occupancy needs and available for free cooling for two weeks in August 2020.

3.2.2. Chiller and AHU Fan Electric Power

To evaluate the electric power associated with the free cooling strategy, models are required to calculate the contribution of chillers and of fans located in the primary and secondary AHU systems. The chiller models developed in Section 3.1.2 were reused for this purpose.

The fan electric power was calculated as a function of flowrate by means of linear regression: the primary AHU fan power is determined from fresh air flowrate; the secondary AHU fan power is estimated from discharged air flowrate. Figure 8 shows the results for the AHU fan power.

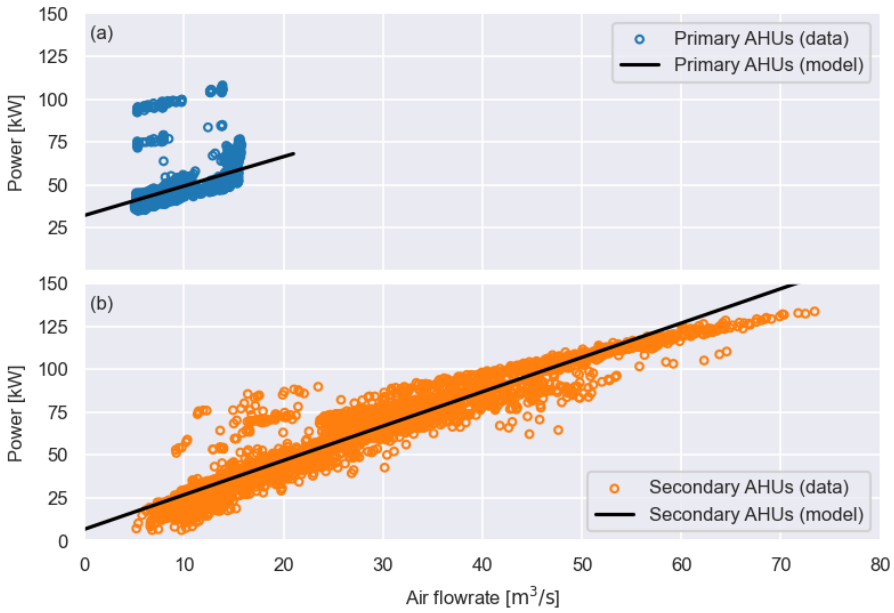

Figure 8. (**a**) Primary AHU fan power as a function of fresh air flowrate; (**b**) secondary AHU fan power as a function of discharged air flowrate.

Under free cooling, a portion of the cooling load can be satisfied by incorporating more fresh air into the ventilation system. This portion is calculated from Equation (9) and the primary AHU system operates at the maximum fresh air flowrate. The rest of the cooling load is supplied by the chillers, which operate at a lower part–load ratio. If the building cooling load is low, it might occur that the entire load can be satisfied by free cooling and the primary AHU system might need to modulate the fresh air flowrate to avoid any overcooling in the building. The total fresh air flowrate becomes the contribution of the fresh air flowrate for occupancy needs and for free cooling. In contrast, the discharged air flowrate depends on the building cooling load; Figure 9 shows this behavior under the baseline operation as well as the obtained model. Based on the model, the total discharged air flowrate under the free cooling mode was calculated as the sum of the additional fresh air flowrate and the discharged air flowrate at the cooling load covered by the chillers (i.e., total building cooling load minus free cooling thermal power). Note that the contribution of increased fan power to the building cooling load was neglected for simplicity.

Table 3 shows the accuracy of the fan power models and discharged air flowrate model based on R^2, NMBE, and CV-RMSE [39]. The results are given in Table 3 and show good consistency with the operational data.

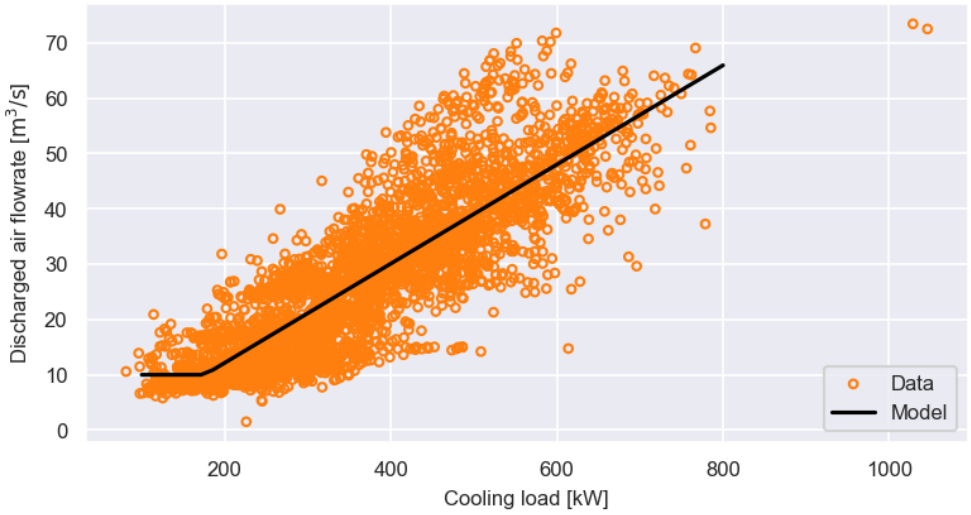

Figure 9. Discharged air flowrate as a function of the cooling load from the chilled water system under baseline operation.

Table 3. Accuracy of fan power and discharged air flowrate models.

Variable	Model	R^2	NMBE	CV-RMSE
Primary AHU fan power	Linear	0.22	-3.6×10^{-14}%	22.4%
Secondary AHU fan power	Linear	0.91	3.1×10^{-14}%	14.8%
Discharged air flowrate	Linear	0.73	0.65%	27.9%

3.2.3. Proposed Free Cooling Strategy

The free cooling thermal power given in Equation (9) mainly depends on the difference between indoor air (approximated by exhaust air) and outdoor air conditions: the larger the difference, the higher the free cooling thermal power. However, this does not guarantee that it is always energy efficient to run the building under free cooling conditions. It is therefore required to verify that the sum of the electric power of the chilled water system and that of the AHU fans is reduced compared to the baseline case. Figure 10 depicts the reduction in total electric power of the chilled water system and AHU fans as a function of the enthalpy difference between indoor and exhaust air. The negative values indicate that operating under free cooling increases the electric power. From this figure, we can clearly see a change point at 7.5 kJ/kg from which the electric power reduction becomes positive and free cooling thus becomes energy efficient. It is worth mentioning that this change point was obtained with the chiller sequencing under baseline operation; nonetheless, it does not change with the proposed chiller sequencing strategy.

The outdoor air conditions that allow for efficient free cooling were investigated and the results are shown in Figure 11. It can be clearly seen that the temperature is the main driver for efficient free cooling; however, relative humidity also plays an important role. Overall, free cooling was found to be effective when the outdoor air temperature was lower than 21 °C; however, the threshold also depends on relative humidity and a free cooling strategy based on outdoor air temperature only could have increased the electric power. Such a strategy could become quite effective during shoulder seasons when, for instance, outdoor air temperature at night can be low while cooling is still required for the building to compensate for internal gains.

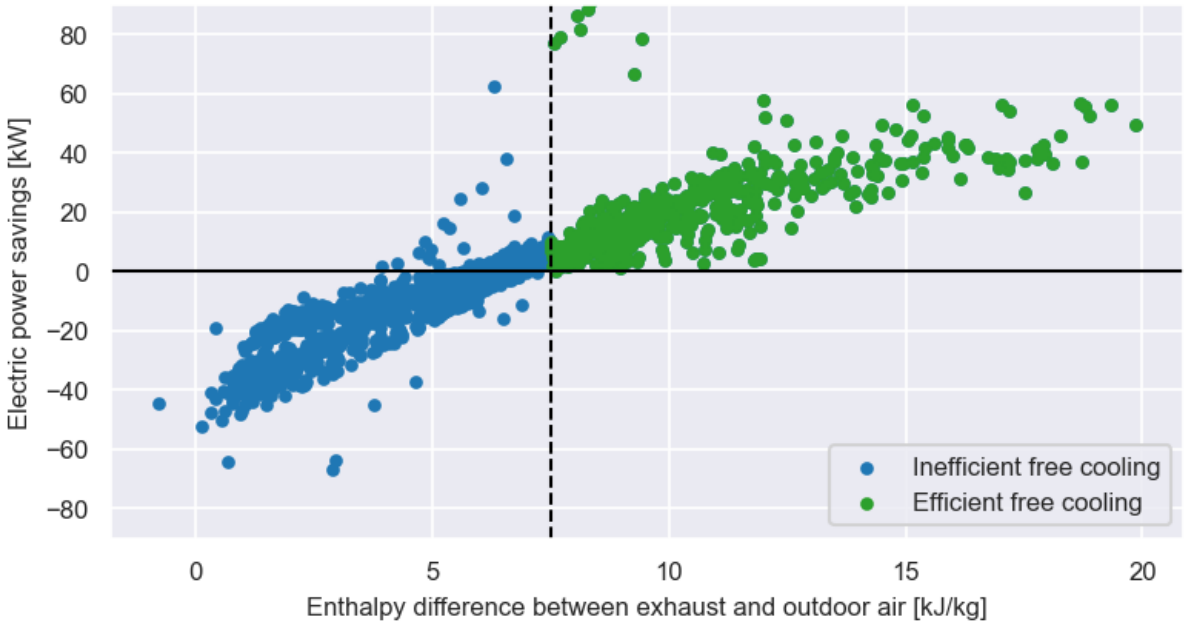

Figure 10. Reduction in total electric power of chilled water system and AHU fans by using free cooling as a function of the enthalpy difference between exhaust and outdoor air.

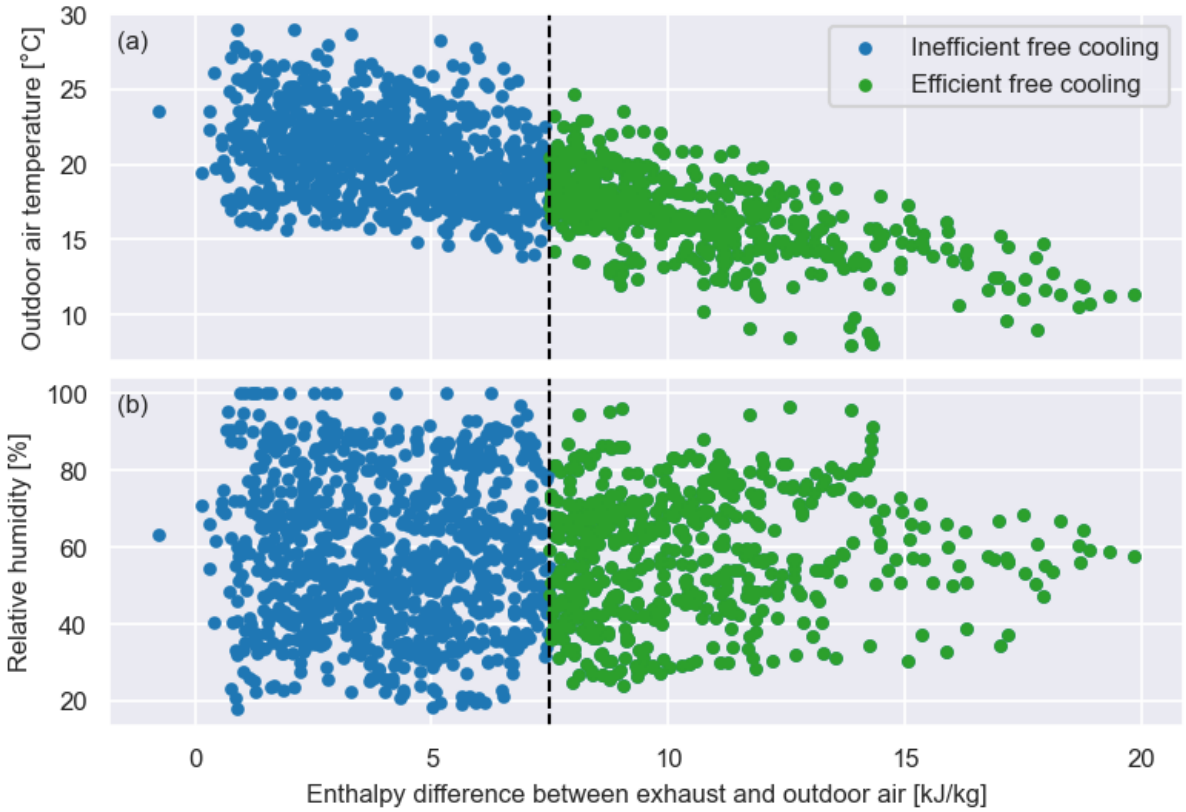

Figure 11. (**a**) Outdoor air temperature and (**b**) relative humidity for inefficient and efficient free cooling as a function of the enthalpy difference between exhaust and outdoor air.

Such a global approach not only makes the proposed free cooling strategy applicable to conventional HVAC configurations with economizers but also to more unique configurations. It requires chiller and fan electric power and fresh air flowrates, and allows for evaluation of the overall benefits of the proposed free cooling strategy. In terms of implementation, the proposed strategy is simple and could be easily implemented by using

the enthalpy difference between exhaust and outdoor air, and the estimated threshold of 7.5 kJ/kg.

3.3. Supply Air Temperature Reset

3.3.1. Proposed Supply Air Temperature Reset Strategy

To improve AHU energy efficiency in a VAV system, Supply Air Temperature (SAT) setpoint is a common variable to optimize. ASHRAE G36 [31] has recommended various SAT reset strategies for AHUs. Zhang et al. [18] reported that the G36 SAT reset strategy based on outdoor dry bulb temperature saved energy in different California climates.

The existing SAT setpoints for the two AHUs in the case study are configured to be constantly equal to 13 °C. This low setpoint requests cooling load from the chillers as long as the outdoor air (close to cooling coil inlet temperature) is higher than the setpoint value due to the lack of air economizers in the AHUs (see Figure 2). This generates an unnecessary cooling load for the chillers even when the outdoor air is relatively cool and dry, especially during shoulder seasons or cold summer nights. G36 suggests resetting SAT setpoint to a higher value when the outdoor air is in favorable conditions. Specifically, it recommends adjusting the SAT setpoint proportionally from 13 °C to 18 °C when the outdoor air changes from 21 °C to 16 °C [31].

To consider the impact of humidity, this work adopts a reset strategy based on outdoor air enthalpy. The green line in Figure 12 shows the proposed SAT reset strategy based on fixed outdoor air enthalpy. The SAT setpoint range is selected to be the same as that in G36 from 13 °C to 18 °C. The low and high limits for the outdoor air enthalpy (40.5 kJ/kg and 61.6 kJ/kg, respectively) are selected by considering the same outdoor dry bulb temperature (16 and 21 °C) with a constant relative humidity at 85%. Note that this high limit of outdoor air enthalpy, 61.6 kJ/kg, is lower than the high limit, 65.1 kJ/kg (equivalent to 24 °C outdoor air at 85% relative humidity), specified in ASHRAE Standard 90.1 [34] for an air economizer based on fixed enthalpy with a fixed dry bulb temperature of outdoor air for all ASHRAE climate zones. It is, therefore, considered to be safe for the proposed SAT reset strategy not to introduce extra humidity into the building.

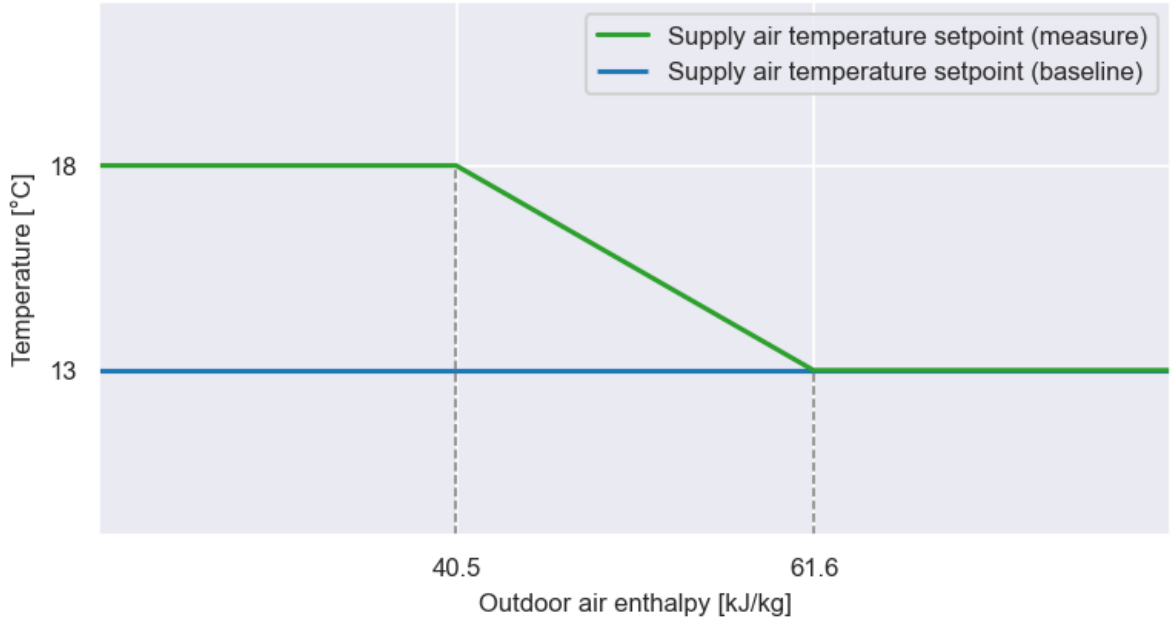

Figure 12. Proposed supply air temperature reset strategy as a function of outdoor air enthalpy while the existing supply air temperature setpoint remains constant.

3.3.2. AHU Cooling Load Calculation

To evaluate the cooling load reduction in the SAT reset strategy, it is necessary to calculate the cooling load of the coils in the AHUs. The BAS measures and stores the temperature, relative humidity, and flowrates of the fresh air, as well as the inlet and outlet temperatures of the cooling coils. Based on mass and energy balance equations [36,41], the cooling coil load of an AHU can be calculated using Equation (10):

$$q_{\text{AHU}} = \dot{m}_{a,AHU_i}(h_a(T_{\text{coil,i,in}}, \omega_{\text{coil,i,in}}) - h_a(T_{\text{coil,i,out}}, \omega_{\text{coil,i,out}})) - \dot{m}_{w,AHU_i} h_w(T_{\text{coil,i,out}}, x = 0), \quad (10)$$

where $\dot{m}_{a,AHU_i}$ and $\dot{m}_{w,AHU_i}$ are the mass flow rate of air and condensation water in AHU$_i$; indices *coil*,*i*,*in* and *coil*,*i*,*out* refer to the cooling coil inlet and outlet of AHU$_i$. h_a is the enthalpy of the humid air, and h_w is the water condensation from the humid air. T and ω are the temperature and humidity ratio, and x is vapor quality.

For the calculation of the baseline cooling load, the measured values were used for the outlet temperatures of the cooling coils. For the calculation of the cooling load with the reset strategy, the outlet temperatures of the cooling coils were assumed to be equal to the SAT reset setpoints. This assumption is considered to be reasonable, as the existing data of the SAT and its setpoint show negligible discrepancies. In other words, the cooling coils were always able to deliver the required cooling load within the sampling rate (5 min) of the data and there was no risk that the reset setpoint could not be reached or would be reached with significant delay.

The proposed temperature reset strategy follows a structure commonly found in BAS and generally implemented through if/then statements, which eases its implementation. Moreover, such a strategy could be replicated to other HVAC configurations with primary/secondary AHUs, as well as different AHU configurations with small modifications, as proposed by G36.

3.4. Methodology to Assess Performance

The performance of each measure was first evaluated individually, and a baseline case (reference or BAU, "Business As Usual") was defined to evaluate energy savings. It consists of: (a) the measured building cooling load (i.e., no SAT reset strategy), which is fully satisfied by the cooling system (i.e., no free cooling), whose electric power is calculated using the chiller models; (b) a baseline chiller sequencing deduced from the measured operation (i.e., which chiller in operation at a given time); and (c) measured fresh air flowrates and discharged air flowrates to calculate fan electric power (i.e., no free cooling). Once the individual assessment was performed, the impact of all measures together was evaluated. In summary, this means:

- *Chiller sequencing*: the new chiller sequencing was compared with the baseline sequencing for the same building cooling load without free cooling;
- *Free cooling strategy*: the proposed free cooling strategy was compared to the baseline case without free cooling for the same building cooling load and chiller sequencing;
- *Supply air temperature reset strategy*: the SAT reset strategy was compared with the baseline cooling load for the same chiller sequencing and without free cooling;
- *All measures together*: the air temperature reset strategy coupled with the proposed chiller sequencing and the free cooling strategy were compared with the baseline case.

To assess the energy savings, the decrease in building cooling energy ($\Delta Q_{\text{measure}}$) and the overall reduction in the cooling system electric power ($\Delta W_{\text{measure}}$) were estimated over a given period of time as shown in Equations (11) and (12). For the specific case of free cooling, the cooling system electric power reduction comes along with an increase in AHU

fan power; this effect is considered in the energy savings by penalizing the cooling system electric power reduction with the fan power increase as follows:

$$\Delta Q_{\text{measure}} = \frac{\int_t \left(\dot{Q}_{cool}^{ref} - \dot{Q}_{cool}^{meas} \right) dt}{\int_t \dot{Q}_{cool}^{ref} dt}, \tag{11}$$

$$\Delta W_{\text{measure}} = \frac{\int_t \left(\left(\dot{W}_{cool,sys}^{ref} - \dot{W}_{cool,sys}^{meas} \right) + \left(\dot{W}_{fan}^{ref} - \dot{W}_{fan}^{meas} \right) \right) dt}{\int_t \dot{W}_{cool,sys}^{ref} dt}, \tag{12}$$

where $\dot{Q}_{cool}^{ref}$, $\dot{W}_{cool,sys}^{ref}$, and $\dot{W}_{fan}^{ref}$ are, respectively, the building cooling energy, the cooling system electric power, and the AHU fan power for the baseline case. $\dot{Q}_{cool}^{meas}$, $\dot{W}_{cool,sys}^{meas}$, and $\dot{W}_{fan}^{meas}$ are the same variables for the evaluated measure(s).

4. Performance Evaluation of Data-Driven Measures

The performances of the proposed data-driven measures are given in Table 4 with their associated thermal and electric energy savings. These results are discussed in detail in the sub-sections.

Table 4. Performance of proposed data-driven measures.

Measure	Thermal Energy (Baseline)	Thermal Energy (Measure)	Electric Energy (Baseline)	Electric Energy (Measure)
Chiller sequencing only	1429 MWh	1429 MWh (-)	676 MWh	547 MWh (−19.1%)
Free cooling only	128 MWh	128 MWh (-)	73 MWh	53 MWh (−27.2%)
Supply air temperature reset only	1264 MWh	1103 MWh (−12.7%)	614 MWh	558 MWh (−9.1%)
All measures together	1429 MWh	1261 MWh (−11.8%)	676 MWh	456 MWh (−32.5%)

4.1. Performance of Individual Measures

4.1.1. Chiller Sequencing

The performance of the proposed chiller sequencing was evaluated when one of the chiller combinations described in Section 3.1 was in operation (i.e., for which models were developed) and when data were available (i.e., no missing values). It corresponds to 89% of the whole period.

The new strategy allowed for reducing the cooling system electric power by 19% compared to the baseline case. This was mainly due to the low performance of chiller #1, which was used alone or in combination with the other chillers. From the performance curves shown in Figure 6, operating chillers #2 or #3 was also more energy efficient than the operation of both at the same time. The proposed chiller sequencing extended the operation of individual chillers, which further improved the performance. Figure 13 shows the chiller sequencing for the baseline case and the proposed strategy for two weeks in August 2020. We can see that chiller #1 is not operated anymore while chiller #2 is the most used, especially when the building cooling load is lower than 550–575 kW.

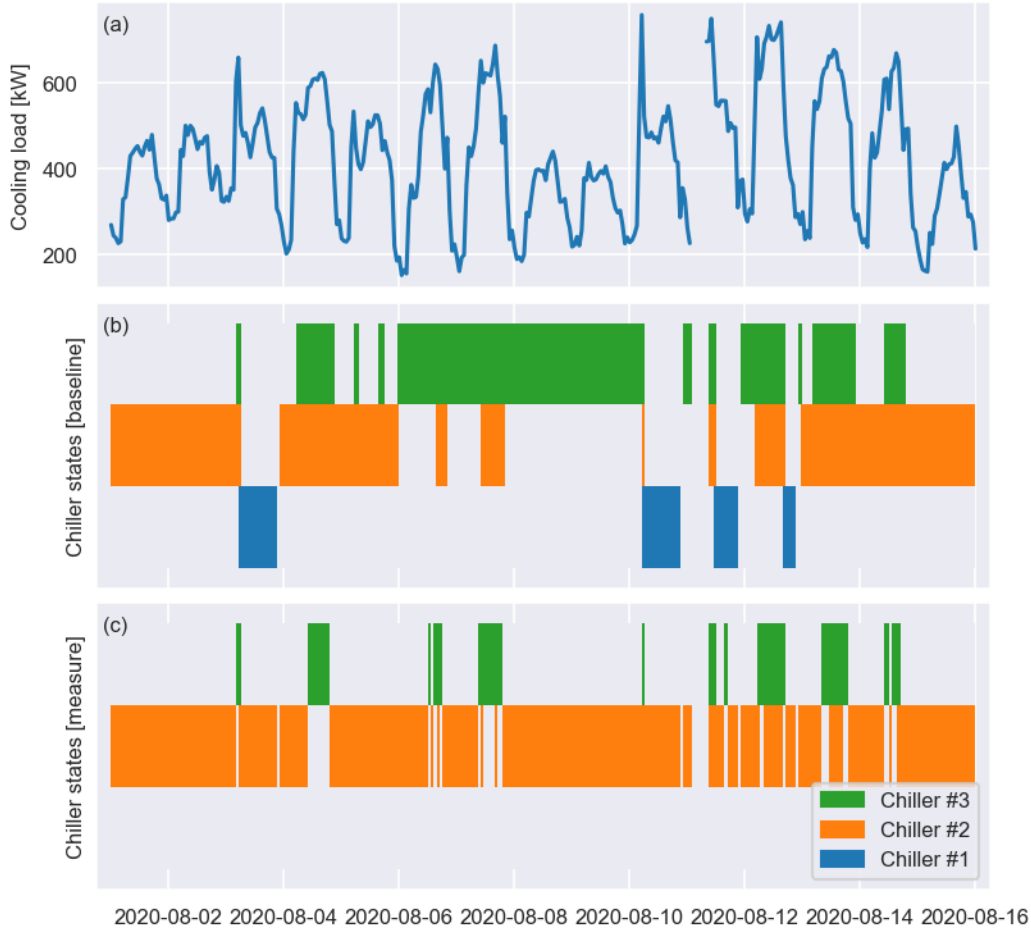

Figure 13. (**a**) Building cooling load, (**b**) baseline chiller sequencing, and (**c**) proposed chiller sequencing for a two-week period.

4.1.2. Free Cooling

To operate under free cooling mode, the building must satisfy two conditions: (a) there must be potential for free cooling (i.e., $\dot{Q}_{\text{free cooling}}$ in Equation (9) higher than zero), and (b) free cooling must be energy efficient (i.e., enthalpy difference between exhaust and outdoor air higher than 7.5 kJ/kg). During the six-month period, free cooling was possible for 33% of the time and efficient free cooling represents 37% of the period when free cooling was possible. Since outdoor air conditions must be favorable, applying the free cooling measure during shoulder seasons (e.g., May and September) would further increase its use.

Although it was not often used during the whole period (12%), Table 4 shows that efficient free cooling can provide significant savings by reducing chilled water system electric energy by 27%. Note that this number includes the increased fan power when the building operates under free cooling mode. Figure 14 shows the results for a one-week period. We can see that free cooling is generally used at night, when outdoor air temperature is cooler and occupancy fresh air requirements are lower; however, it can also be used during the day (e.g., 10 or 16 June). Figure 14b shows the electric power reduction when the building is under free cooling mode. We can clearly see that free cooling helps reduce cooling system electric power when the chilled water system is not required anymore (i.e., at night). When free cooling complements the chilled water system, interesting savings are still achieved.

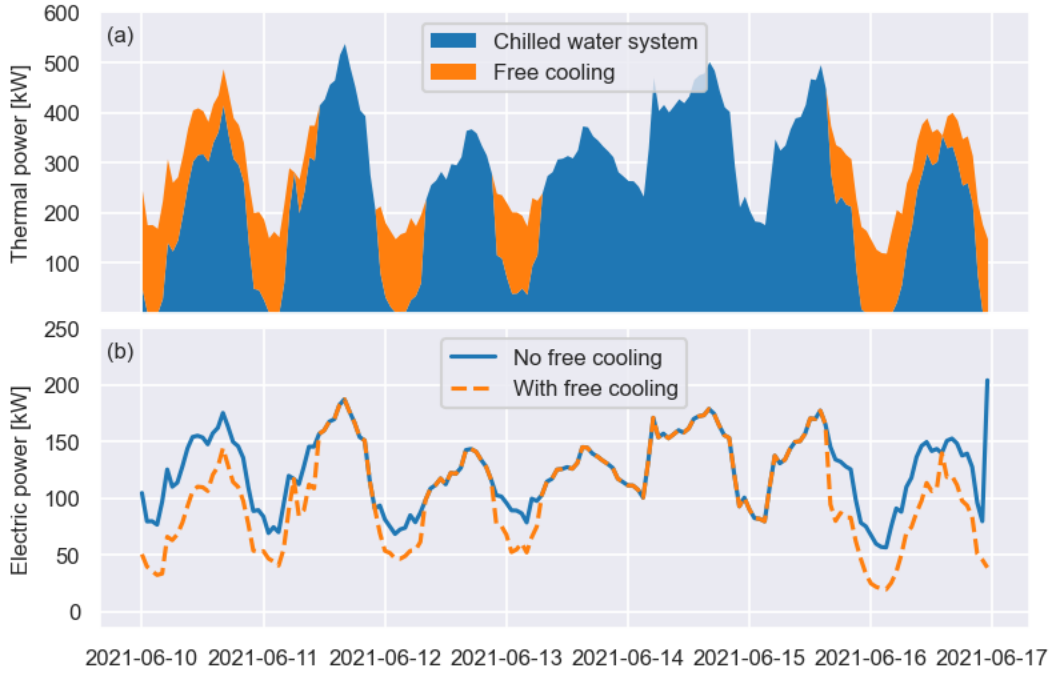

Figure 14. (**a**) Building cooling load satisfied by chilled water system or free cooling and (**b**) electric power with and without free cooling for a one-week period. The electric power is the contribution of the chilled water system power and the increased fan power, as given in Equation (12).

4.1.3. Supply Air Temperature Reset

Figure 15 shows the cooling load of the baseline and proposed reset strategy for a typical week in summer 2021. We can see that the proposed strategy requires less cooling when the outdoor air enthalpy is low, which is especially effective during 1–5 July. Low enthalpy means that the outdoor air is cool and dry during those periods, which leads to less need for the AHU system to further cool and dehumidify the fresh air entering the system. Unlike the existing control, the proposed measure resets the SAT setpoint to a higher value in those conditions and thus reduces the cooling load.

It is worth mentioning that the cooling load was estimated using air-side measurements at the AHU level and might lead to slightly different cooling load results compared to using chilled water measurements in Equation (2), which were used for the chiller sequencing measure. When combined measures are assessed, this cooling load reduction (absolute value) is used along with Equation (2). For more information about the differences and uncertainties regarding the two cooling load calculation methods, see [36,41].

Figure 16 summarizes the average cooling load of the baseline and proposed SAT measure for the two summers. We can see that the measure was able to reduce cooling load for all summer months by 7–22%, with slightly more reductions in June. It was expected that the measure could further reduce the cooling load in shoulder seasons such as in the months of May and September. The overall cooling load reduction from the SAT measure is 12.7% against the baseline for the investigated six months as shown in Table 4. The decrease in cooling energy comes along with a reduced utilization of the chilled water system and a reduction in electric power, estimated at 9.1%.

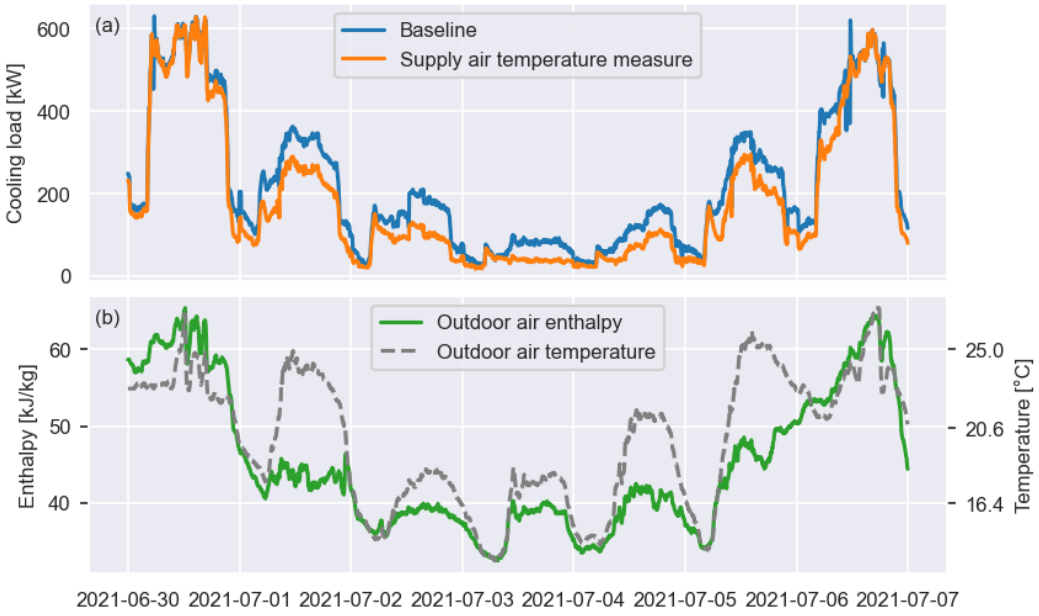

Figure 15. (**a**) Cooling load of a typical week in 2021 for the baseline and proposed supply air temperature reset strategy; (**b**) outdoor air enthalpy and dry bulb temperature for the same week.

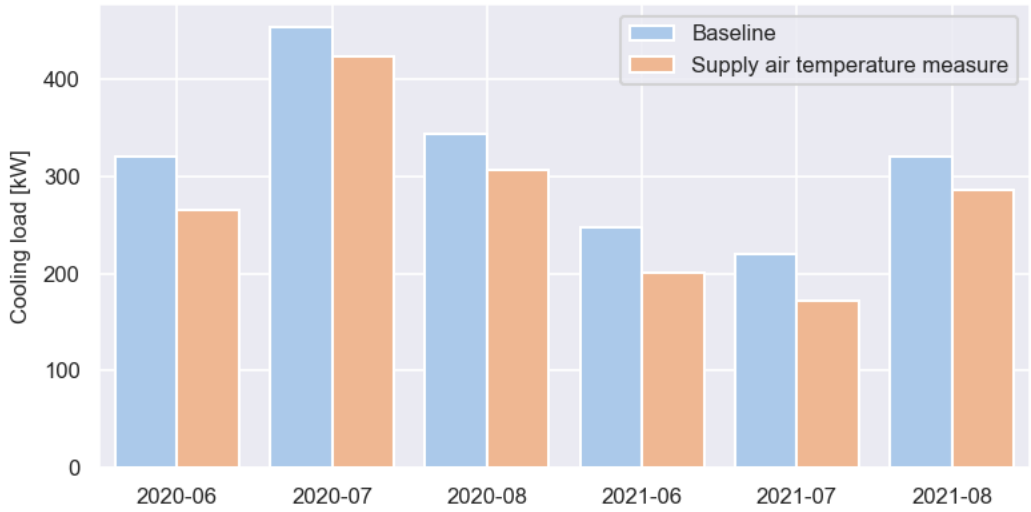

Figure 16. Average cooling load per month for the baseline and proposed supply air temperature reset strategy during 2020 and 2021 summer.

4.2. Performance of Combined Measures

The combined effect of all of the measures applied together is given in Table 4. It shows an overall reduction in thermal energy of 11.8% and in electric energy of 32.5%. The SAT reset strategy allows for reducing both the thermal and electric energy. The new chiller sequencing takes advantage of the most energy-efficient chillers and directly tackles chilled water system electric power. Finally, when effective, the free cooling strategy permits further reducing electric energy by increasing fresh air intake into the building, thus reducing the usage of the chilled water system.

Figure 17 shows the cooling load and electric power for the baseline and the combined measures for a typical week in 2021. Both thermal and electric power are consistently reduced due to the combined effects of chiller sequencing, free cooling, and SAT reset strategies.

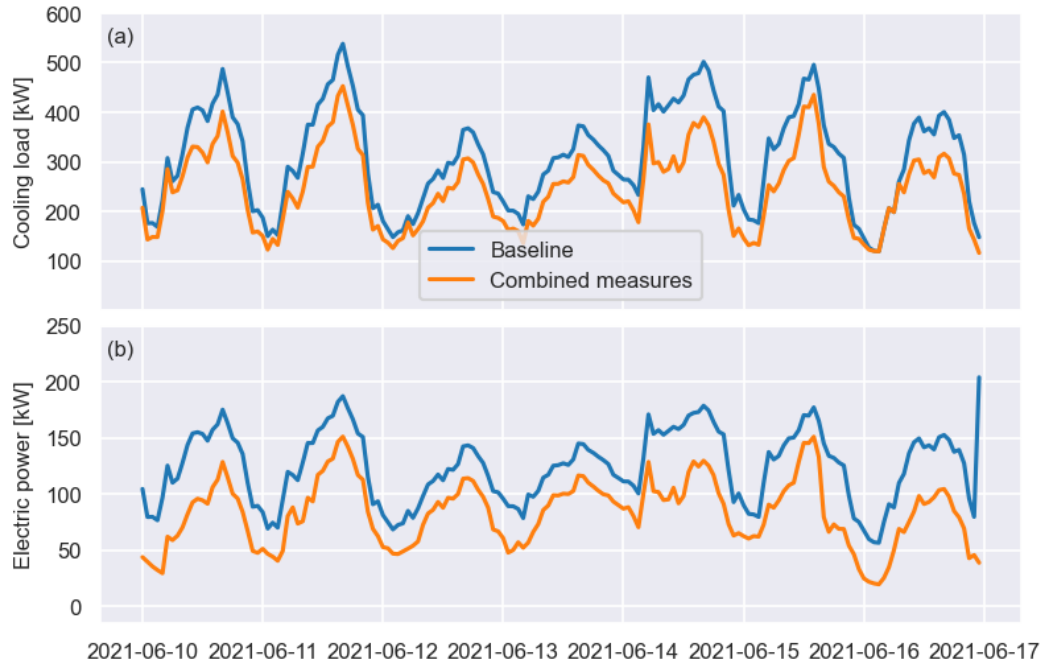

Figure 17. (**a**) Building cooling load; (**b**) electric power for the baseline and the combined measures for a typical week. The electric power is the contribution of the chilled water system power and the increased fan power, as given in Equation (12).

On a monthly basis, Figure 16 shows the cooling load reduction of the SAT reset strategy; however, it also represents the results of the combined measures, since only the SAT reset strategy affects the building cooling load. For the chilled water system electric power, Figure 18 shows the average monthly results and reductions ranging between 23% and 46%. In 2020, June provideed higher savings (34%) due to the most favorable outdoor air conditions, which allowed for operating under the effective SAT reset strategy and free cooling mode. In 2021, more significant savings were achieved, especially for the months of July and August (36–46%). These savings were mainly achieved due to the new chiller sequencing, which avoids the usage of both the chiller #1 alone and the chillers #1-3, which show poor performance, as displayed in Figure 6.

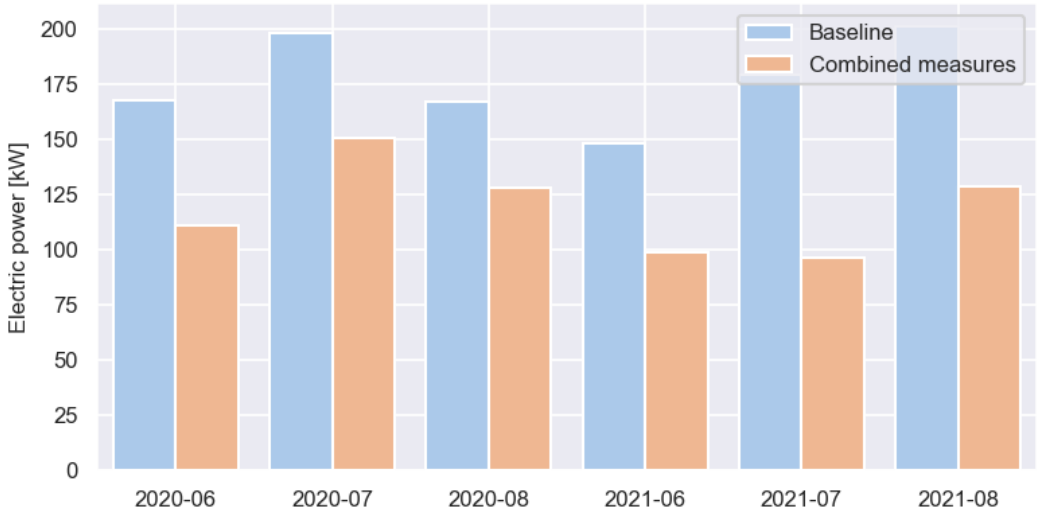

Figure 18. Average chilled water system electric power per month for the baseline and the combined measures during summer 2020 and 2021.

4.3. Generalizability of Proposed Data-Driven Measures

The proposed data-driven measures were built on models to obtain insights into the cooling system performance to further optimize building operation. To facilitate the implementation in the current control system, the proposed measures were aimed to be implemented by means of simple rule-based controls:

- *Chiller sequencing*: the sequencing can be implemented using switch-on and switch-off thresholds as given in Table 2; this sequence could act as a master controller and could be further overridden by local control rules if required (e.g., a high temperature limit can be reached, which may require a chiller switch). This strategy could be replicated to any other multi-chiller systems with the same ease of implementation.
- *Free cooling*: the free cooling mode requires the change point (7.5 kJ/kg, as shown in Figure 10) and the enthalpy calculations for both exhaust and outdoor air; the library Coolprop [42] can be used for this purpose. Additional control modifications are necessary to allow the fresh air flowrate to increase. This strategy could not only be replicated to conventional HVAC configurations with economizers, but also to more unique configurations.
- *Supply air temperature reset*: reset strategies are already commonly used in BAS for various temperatures with if/then statements. The proposed temperature reset strategy is given in Figure 12 and relies on outdoor air enthalpy estimation; the library Coolprop [42] can be used in this case as well. This strategy is inspired by ASHRAE Guideline 36 [31] and, as such, it could be replicated to many AHU systems with minor adjustments.

The proposed measures could be generalized to other buildings; however, their development depends on the available operational data while the tuning of control parameters (i.e., chiller sequencing switch-on and switch-off thresholds, free cooling change point, temperature reset strategy parameters) requires careful data analysis and model development.

5. Conclusions

This work tackled the development of three data-driven model-based control strategies to improve the cooling performance of commercial and institutional buildings:

- A new chiller sequencing based on data-driven performance curves;
- A free cooling strategy considering both chilled water system electric power and air handling unit fan power;
- A supply air temperature reset strategy based on outdoor air enthalpy.

These measures were built upon operational data and virtual energy meters and models, and were intended to be relatively simple to develop and easy to implement in actual control systems. This approach makes the proposed measures more robust and less prone to errors compared to more complex methods because the installation of additional hardware is not required, which makes the approach more easily replicable in other buildings.

These measures were developed for an existing large commercial building and were evaluated both individually and all together during summer (June–August) 2020 and 2021. The results showed that the chiller sequencing could reduce chilled water system electric energy by 19%. The free cooling strategy was efficient with a 27% reduction in electric energy; however, this mode could be activated during only a small fraction of the summer periods (12%). More energy savings would be expected by extending the analysis to shoulder seasons (e.g., May and September). Finally, the supply air temperature reset strategy helped to reduce the building cooling load by 13% and, as a side effect, reduced the electric power by 9%. All of the measures combined allowed for a reduction in building cooling load by 12% and chilled water system electric power by 33% over the six months studied.

Future work includes field implementation of the proposed measures in the case study building, replication to other existing buildings, and the development of a predic-

tive control strategy built upon the proposed measures to further improve the building cooling performance.

Author Contributions: E.S.: Conceptualization, Methodology, Software, Validation, Formal analysis, Data Curation, Writing—original draft, Writing—review & editing, Visualization, Project administration. K.Z.: Conceptualization, Methodology, Software, Validation, Formal analysis, Data Curation, Writing—original draft, Writing—review & editing, Visualization. All authors have read and agreed to the published version of the manuscript.

Funding: The authors want to gratefully acknowledge the financial support of Natural Resources Canada through the Office of Energy Research and Development.

Data Availability Statement: Data not available due to privacy restrictions.

Acknowledgments: The authors would like to thank our external partners for sharing their experience, providing data and feedback, and internal and external reviewers for their useful comments.

Conflicts of Interest: The authors declare no conflict of interest.

References

1. Fernandez, N.; Katipamula, S.; Wang, W.; Xie, Y.; Zhao, M.; Corbin, C. *Impacts of Commercial Building Controls on Energy Savings and Peak Load Reduction*; Pacific Northwest National Laboratory, U.S. Department of Energy: Richland, WA, USA, 2017.
2. Li, X.; Wen, J. Review of Building Energy Modeling for Control and Operation. *Renew. Sustain. Energy Rev.* **2014**, *37*, 517–537. [CrossRef]
3. U.S. Green Building Council Benefits of Green Building. Available online: https://www.usgbc.org/articles/benefits-green-building (accessed on 16 September 2022).
4. Kramer, H.; Lin, G.; Curtin, C.; Crowe, E.; Granderson, J. *Proving the Business Case for Building Analytics*; Lawrence Berkeley National Laboratory: USA, 2020. [CrossRef]
5. Drgoňa, J.; Arroyo, J.; Cupeiro Figueroa, I.; Blum, D.; Arendt, K.; Kim, D.; Ollé, E.P.; Oravec, J.; Wetter, M.; Vrabie, D.L.; et al. All You Need to Know about Model Predictive Control for Buildings. *Annu. Rev. Control.* **2020**, *50*, 190–232. [CrossRef]
6. Cotrufo, N.; Saloux, E.; Hardy, J.M.; Candanedo, J.A.; Platon, R. A Practical Artificial Intelligence-Based Approach for Predictive Control in Commercial and Institutional Buildings. *Energy Build.* **2020**, *206*, 109563. [CrossRef]
7. Saloux, E.; Cotrufo, N.; Candanedo, J. A Practical Data-Driven Multi-Model Approach to Model Predictive Control: Results from Implementation in an Institutional Building. In Proceedings of the 6th International High Performance Buildings Conference, West Lafayette, IN, USA, 28 May 2021.
8. Wang, S.; Ma, Z. Supervisory and Optimal Control of Building HVAC Systems: A Review. *HVACR Res.* **2008**, *14*, 3–32. [CrossRef]
9. Afram, A.; Janabi-Sharifi, F. Theory and Applications of HVAC Control Systems–A Review of Model Predictive Control (MPC). *Build. Environ.* **2014**, *72*, 343–355. [CrossRef]
10. Taheri, S.; Hosseini, P.; Razban, A. Model Predictive Control of Heating, Ventilation, and Air Conditioning (HVAC) Systems: A State-of-the-Art Review. *J. Build. Eng.* **2022**, *60*, 105067. [CrossRef]
11. Thieblemont, H.; Haghighat, F.; Ooka, R.; Moreau, A. Predictive Control Strategies Based on Weather Forecast in Buildings with Energy Storage System: A Review of the State-of-the Art. *Energy Build.* **2017**, *153*, 485–500. [CrossRef]
12. Yu, Z.; Huang, G.; Haghighat, F.; Zhang, G. Control Strategies for Integration of Thermal Energy Storage into Buildings: State-of-the-Art Review. *Energy Build.* **2015**, *106*, 203–215. [CrossRef]
13. Péan, T.Q.; Salom, J.; Costa-Castelló, R. Review of Control Strategies for Improving the Energy Flexibility Provided by Heat Pump Systems in Buildings. *J. Process Control.* **2019**, *74*, 35–49. [CrossRef]
14. Darwazeh, D.; Duquette, J.; Gunay, B.; Wilton, I.; Shillinglaw, S. Review of Peak Load Management Strategies in Commercial Buildings. *Sustain. Cities Soc.* **2021**, *77*, 103493. [CrossRef]
15. Mirakhorli, A.; Dong, B. Occupancy Behavior Based Model Predictive Control for Building Indoor Climate—A Critical Review. *Energy Build.* **2016**, *129*, 499–513. [CrossRef]
16. Park, J.Y.; Ouf, M.M.; Gunay, B.; Peng, Y.; O'Brien, W.; Kjærgaard, M.B.; Nagy, Z. A Critical Review of Field Implementations of Occupant-Centric Building Controls. *Build. Environ.* **2019**, *165*, 106351. [CrossRef]
17. Shi, Z.; Newsham, G.; Ashouri, A.; Pardasani, A. Comparative Study of Pre-Cooling Strategies for Houses in Southern Ontario. In Proceedings of the 11th eSim Building Simulation Conference, Vancouver, BC, Canada, 14–16 June 2021.
18. Zhang, K.; Blum, D.; Cheng, H.; Paliaga, G.; Wetter, M.; Granderson, J. Estimating ASHRAE Guideline 36 Energy Savings for Multi-Zone Variable Air Volume Systems Using Spawn of EnergyPlus. *J. Build. Perform. Simul.* **2022**, *15*, 215–236. [CrossRef]
19. Raman, N.; Chen, B.; Barooah, P. A Unified MPC Formulation for Control of Commercial HVAC Systems in Multiple Climate Zones. In Proceedings of the International High Performance Buildings Conference, West Lafayette, IN, USA, 24–28 May 2021.
20. Hobson, B.W.; Gunay, H.B.; Ashouri, A.; Newsham, G.R. Occupancy-Based Predictive Control of an Outdoor Air Intake Damper: A Case Study. In Proceedings of the eSim 2020: 11th Conference of IBPSA-Canada, Vancouver, BC, Canada, 14–16 June 2020; p. 8.

21. Yuan, S.; Vallianos, C.; Athienitis, A.; Rao, J. A Study of Hybrid Ventilation in an Institutional Building for Predictive Control. *Build. Environ.* **2018**, *128*, 1–11. [CrossRef]
22. Vallianos, C.; Athienitis, A.; Rao, J. Hybrid Ventilation in an Institutional Building: Modeling and Predictive Control. *Build. Environ.* **2019**, *166*, 106405. [CrossRef]
23. Thangavelu, S.R.; Myat, A.; Khambadkone, A. Energy Optimization Methodology of Multi-Chiller Plant in Commercial Buildings. *Energy* **2017**, *123*, 64–76. [CrossRef]
24. Liao, Y.; Huang, G. A Hybrid Predictive Sequencing Control for Multi-Chiller Plant with Considerations of Indoor Environment Control, Energy Conservation and Economical Operation Cost. *Sustain. Cities Soc.* **2019**, *49*, 101616. [CrossRef]
25. Gunay, H.B.; Ashouri, A.; Shen, W. Load Forecasting and Equipment Sequencing in a Central Heating and Cooling Plant: A Case Study. *ASHRAE Trans.* **2019**, *125*, 513–523.
26. Liu, S.; Henze, G.P. Experimental Analysis of Simulated Reinforcement Learning Control for Active and Passive Building Thermal Storage Inventory: Part 1. Theoretical Foundation. *Energy Build.* **2006**, *38*, 142–147. [CrossRef]
27. Candanedo, J.A.; Dehkordi, V.R.; Stylianou, M. Model-Based Predictive Control of an Ice Storage Device in a Building Cooling System. *Appl. Energy* **2013**, *111*, 1032–1045. [CrossRef]
28. Song, X.; Zhu, T.; Liu, L.; Cao, Z. Study on Optimal Ice Storage Capacity of Ice Thermal Storage System and Its Influence Factors. *Energy Convers. Manag.* **2018**, *164*, 288–300. [CrossRef]
29. Feng, J. (Dove); Chuang, F.; Borrelli, F.; Bauman, F. Model Predictive Control of Radiant Slab Systems with Evaporative Cooling Sources. *Energy Build.* **2015**, *87*, 199–210. [CrossRef]
30. Pang, X.; Duarte, C.; Haves, P.; Chuang, F. Testing and Demonstration of Model Predictive Control Applied to a Radiant Slab Cooling System in a Building Test Facility. *Energy Build.* **2018**, *172*, 432–441. [CrossRef]
31. American Society of Heating, Refrigeration and Air Conditioning Engineers. ASHRAE Guideline 36-2021 High-Performance Sequences of Operation for HVAC Systems; ASHRAE: Atlanta, GA, USA, 2021. Available online: https://www.techstreet.com/ashrae/standards/guideline-36-2021-high-performance-sequences-of-operation-for-hvac-systems?product_id=2229690 (accessed on 25 January 2023).
32. Fan, B.; Jin, X.; Du, Z. Optimal Control Strategies for Multi-Chiller System Based on Probability Density Distribution of Cooling Load Ratio. *Energy Build.* **2011**, *43*, 2813–2821. [CrossRef]
33. Chen, Y.; Yang, C.; Pan, X.; Yan, D. Design and Operation Optimization of Multi-Chiller Plants Based on Energy Performance Simulation. *Energy Build.* **2020**, *222*, 110100. [CrossRef]
34. *90.1-2019*; American Society of Heating, Refrigeration and Air Conditioning Engineers ANSI/ASHRAE/IES Standard—Energy Standard for Buildings Except Low-Rise Residential Buildings. ASHRAE: Atlanta, GA, USA, 2019. Available online: https://www.ashrae.org/technical-resources/bookstore/standard-90-1 (accessed on 25 January 2023).
35. Stasi, R.; Ruggiero, F.; Berardi, U. The Efficiency of Hybrid Ventilation on Cooling Energy Savings in NZEBs. *J. Build. Eng.* **2022**, *53*, 104401. [CrossRef]
36. Saloux, E.; Zhang, K. Towards Integration of Virtual Meters into Building Energy Management Systems: Development and Assessment of Thermal Meters for Cooling. *J. Build. Eng.* **2022**, *65*, 105785. [CrossRef]
37. Dou, H.; Zmeureanu, R. Evidence-Based Assessment of Energy Performance of Two Large Centrifugal Chillers over Nine Cooling Seasons. *Sci. Technol. Built Environ.* **2021**, *27*, 1243–1255. [CrossRef]
38. De Coninck, R.; Helsen, L. Practical Implementation and Evaluation of Model Predictive Control for an Office Building in Brussels. *Energy Build.* **2016**, *111*, 290–298. [CrossRef]
39. Afram, A.; Janabi-Sharifi, F. Black-Box Modeling of Residential HVAC System and Comparison of Gray-Box and Black-Box Modeling Methods. *Energy Build.* **2015**, *94*, 121–149. [CrossRef]
40. Lee, W.-S.; Chen, Y.-T.; Kao, Y. Optimal Chiller Loading by Differential Evolution Algorithm for Reducing Energy Consumption. *Energy Build.* **2011**, *43*, 599–604. [CrossRef]
41. Saloux, E.; Zhang, K. Virtual Energy Metering of Whole Building Cooling Load from Both Airside and Waterside Measurements. In Proceedings of the 12th eSim Building Simulation Conference, Ottawa, ON, Canada, 21–24 June 2022.
42. Bell, I.H.; Wronski, J.; Quoilin, S.; Lemort, V. Pure and Pseudo-Pure Fluid Thermophysical Property Evaluation and the Open-Source Thermophysical Property Library CoolProp. *Ind. Eng. Chem. Res.* **2014**, *53*, 2498–2508. [CrossRef]

Disclaimer/Publisher's Note: The statements, opinions and data contained in all publications are solely those of the individual author(s) and contributor(s) and not of MDPI and/or the editor(s). MDPI and/or the editor(s) disclaim responsibility for any injury to people or property resulting from any ideas, methods, instructions or products referred to in the content.